



Divergent and Ultrahigh Thermal Conductivity in Millimeter-Long Nanotubes

Victor Lee,^{1,2} Chi-Hsun Wu,^{1,2} Zong-Xing Lou,^{1,2} Wei-Li Lee,³ and Chih-Wei Chang^{1,*}

¹*Center for Condensed Matter Sciences, National Taiwan University, Taipei 10617, Taiwan*

²*Department of Physics, National Taiwan University, Taipei 10617, Taiwan*

³*Institute of Physics, Academia Sinica, Taipei 11529, Taiwan*

(Received 15 December 2015; published 30 March 2017)

Low-dimensional materials could display anomalous thermal conduction that the thermal conductivity (κ) diverges with increasing lengths, in ways inconceivable in any bulk materials. However, previous theoretical or experimental investigations were plagued with many finite-size effects, rendering the results either indirect or inconclusive. Indeed, investigations on the anomalous thermal conduction must demand the sample length to be sufficiently long so that the phenomena could emerge from unwanted finite-size effects. Here we report experimental observations that the κ 's of single-wall carbon nanotubes continuously increase with their lengths over 1 mm, reaching at least 8640 W/mK at room temperature. Remarkably, the anomalous thermal conduction persists even with the presence of defects, isotopic disorders, impurities, and surface adsorbates. Thus, we demonstrate that the anomalous thermal conduction in real materials can persist over much longer distances than previously thought. The finding would open new regimes for wave engineering of heat as well as manipulating phonons at macroscopic scales.

DOI: 10.1103/PhysRevLett.118.135901

The law of heat transfer in a solid was discovered by Fourier in 1811. Under the steady state, Fourier's law of heat conduction is expressed as

$$J = -\kappa \nabla T, \quad (1)$$

which explicitly states that the heat flux density (J) is proportional to the temperature gradient, and the proportional constant is the thermal conductivity (κ). Empirically, κ is often found to be a constant of a bulk material and is independent of sample geometries. Thus, Fourier's law, together with Ohm's law for electrical conduction and Fick's law for gas diffusion, are traditionally categorized as examples of normal diffusion phenomena.

On the other hand, continuous efforts in seeking solid theoretical grounds for the empirical results have pointed out that anomalous thermal conduction ($\kappa \sim L^\alpha$, $\alpha > 0$, where L is the sample length) could occur in low-dimensional systems [1]. These works, though sometimes referred to as non-Fourier thermal conduction (which, strictly speaking, only applies when the speed of heat conduction cannot be neglected), may be more appropriately described as violations of normal diffusion processes ($\alpha = 0$) in heat conduction. Theoretically, the divergence of κ in one-dimensional systems has been shown to be very robust against disorder or anharmonicity [2–5]. In many models, heat transfer phenomena would depend on the dimensionalities of the system, showing sublinear power-law ($\alpha < 1$) divergence in 1D [1], logarithmic divergence in 2D [6], and normal ($\alpha = 0$) thermal conduction in 3D [7,8]. Apart from the idealized models, it has been suggested that the anomalous thermal conduction could be observed in real systems like single-wall carbon nanotubes (CNTs) [9–17] or graphene ribbons [18]. For example, in a perfect

(i.e., isotopically pure and defect-free) CNT, its κ is predicted to increase sublinearly ($\alpha = 0.33 - 0.5$) with lengths up to millimeters [9,10], characteristically differing from conventional ballistic thermal conduction (i.e., $\alpha = 1$).

However, theoretical disputes on many anomalous effects have not been completely settled yet. For example, while the anomalous thermal conduction is commonplace in many 1D models [19,20], it remains controversial whether a quasi-1D system like a CNT would eventually restore back to normal thermal conduction at finite lengths [9–17]. Experimentally, the formidable challenges in fabricating nanomaterials with very high aspect ratios and the difficulties in measuring their κ 's, combined with unwanted finite-size effects such as fluctuations of defect or disorder densities or conventional ballistic thermal conduction pertinent to micron-sized samples, have plagued many previous experimental observations [21–25].

To rigorously study the fundamental heat transfer phenomena, experimental investigations should be conducted on sufficiently long CNTs. We thus synthesized ultralong single-wall CNTs with lengths exceeding 2 cm using chemical vapor deposition methods [26]. Individual CNTs were picked up by a tailored manipulator and placed on a thermal conductivity test fixture consisting of parallel suspended SiN_x beams, as shown in Fig. 1(a). The suspended SiN_x beams with deposited Pt films were utilized as independent resistive thermometers (RTs) for generating heat or sensing temperature variations. For example, if a Joule heating power (P) is injected at RT_1 [Fig. 1(b)], most of the power will dissipate along RT_1 to the heat bath, following $P_1 = 8\Delta T_1/R_{b1}$ (where R_{b1} is the total thermal resistance of the RT_1 and ΔT_1 is the temperature rise above

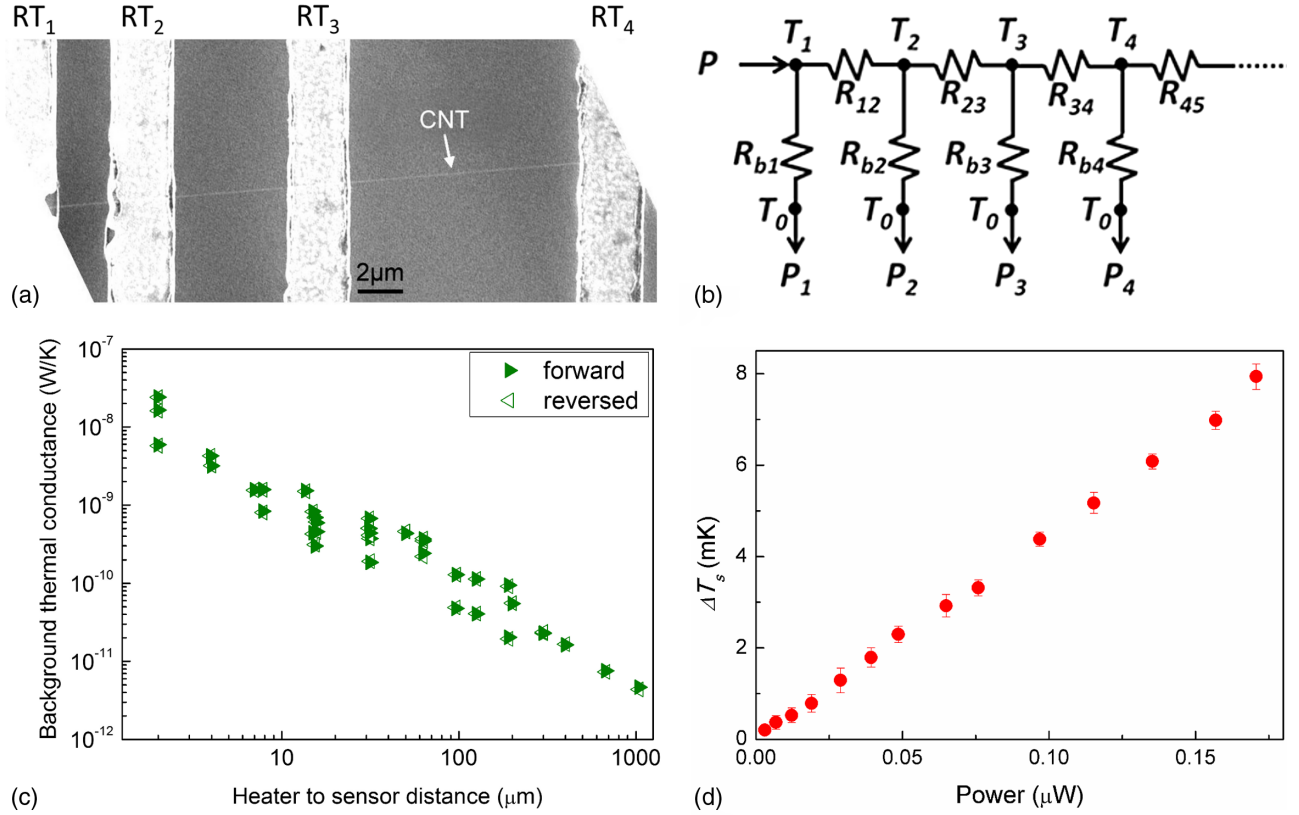


FIG. 1. (a) SEM image of a CNT anchored on a test fixture consisting of parallel resistive thermometers (RT_i 's) made by Pt films on SiN_x beams. (b) The corresponding thermal circuits when RT_1 is used as a heater. (c) Measured background thermal conductance due to radiation heat transfer (from heater to sensor) for various heater-to-sensor distances. The measured values for forward and reversed biases (i.e., exchanging the role of the heater and the sensor) are shown, demonstrating $f_{ij} = 1 \pm 0.04$. We have noticed that the background thermal conductance is sensitive to the environment (such as whether the Si substrate is fully etched through or partially etched), so that the measured values are different even if the heater-to-sensor distances are similar. (d) Measure ΔT_s vs P for driving frequency at 2 Hz, which gives a noise equivalent thermal conductance of $4.7 \times 10^{-12} \text{ W K}^{-1} \text{ Hz}^{-1/2}$ at room temperature.

the heat bath, measured at the middle of RT_1 , where a CNT is anchored). On the other hand, the power flowing through the CNT is the sum of the power measured by individual sensors; i.e., $P_j = 4\Delta T_j/R_{bj}$. Because $P = P_1 + P_2 + P_3 + \dots$, the thermal conductance of the CNT (K_{12}) anchored between RT_1 and RT_2 follows

$$K_{12} = \frac{4\left(\frac{\Delta T_2}{R_{b2}} + \frac{\Delta T_3}{R_{b3}} + \dots\right)}{\Delta T_1 - \Delta T_2} = \frac{P(f_{12}\Delta T_2 + f_{13}\Delta T_3 + \dots)}{(2\Delta T_1 + f_{12}\Delta T_2 + f_{13}\Delta T_3 + \dots)(\Delta T_1 - \Delta T_2)}, \quad (2)$$

where $f_{ij} \equiv R_{bi}/R_{bj}$. The f_{ij} 's can be determined from the asymmetry of background measurement before anchoring a CNT. As shown in Fig. 1(c), we have found that although the measured background thermal conductances varied from $3.18 \times 10^{-9} \text{ W/K}$ to $4.51 \times 10^{-12} \text{ W/K}$ (for heater-to-sensor distance $4 \mu\text{m} - 1.039 \text{ mm}$), they display symmetric results; i.e., $f_{ij} = 1 \pm 0.04$. In addition, the temperature rise of the heater (sensor) is a parabolic (linear) function of the location; thus, we have $\overline{\Delta T} = 2\Delta T_1/3$ and $\overline{\Delta T}_j = \Delta T_j/2$

(where $j = 2, 3, 4, \dots$ and $\overline{\Delta T}_i$ is the average temperature rise of RT_i) [26]. Experimentally, we have found that $\overline{\Delta T}_1 \sim 20 \text{ K} \gg \overline{\Delta T}_2 \gg \overline{\Delta T}_3 \gg \overline{\Delta T}_4$. Thus, the thermal conductance (K_{12}) of a CNT anchored between RT_1 and RT_2 can be expressed by

$$K_{12} = \frac{2P(\overline{\Delta T}_2 + \overline{\Delta T}_3 + \dots)}{3\overline{\Delta T}_1\left(\frac{3}{2}\overline{\Delta T}_1 - \overline{\Delta T}_2\right)}. \quad (3)$$

The above result can be generalized to thermal conductance of a CNT anchored between any neighboring RT_i and RT_j . During the experiment, an alternating current with frequency f ($< 7 \text{ Hz}$) was supplied to the heater (RT_i) and the corresponding changes of the temperature on the sensor (RT_j) were detected at frequency $2f$ using a lock-in amplifier. The background contribution due to radiation heat transfer from the heater to the sensor had been carefully measured and subtracted so as to obtain the thermal conductance of the CNTs on the same device and of identical heater-sensor configurations. As shown in Fig. 1(d), the test fixture is capable of measuring temperature variations

~ 0.28 mK at room temperature (time constant = 10 sec), which is equivalent to a thermal conductance resolution 4.7×10^{-12} WK $^{-1}$ Hz $^{-1/2}$. After the measurement, sections of sample 6 and sample 9 were successfully transferred to a TEM for further characterizations [26]. Unfortunately, due to the vibrations of the long CNTs under TEM imaging, the diameter (d) cannot be precisely measured. We thus assume $d = 2$ nm and thickness $\delta = 0.34$ nm for determining the measured $\kappa_m = KL/\pi d\delta$ of the investigated CNTs. Importantly, the investigated L 's span from few micrometers [Fig. 1(a)] to millimeters (Fig. 2; see also Ref. [26] for SEM images of the investigated CNTs).

Figure 3 shows κ_m vs L relations for nine different CNTs. The L 's of the investigated CNTs span 3 orders of magnitude, varying from 2 μ m to 1.039 mm. Because the diameter and the chirality are less likely to change in an ultralong CNT [27], the uncertainties can be minimized by analyzing the length dependence of κ of the same sample. Remarkably, the measured κ_m 's (open symbols) of sample 2 to sample 9 display unambiguous divergent behavior with increasing L . No divergence of κ_m is observed in sample 1, possibly due to

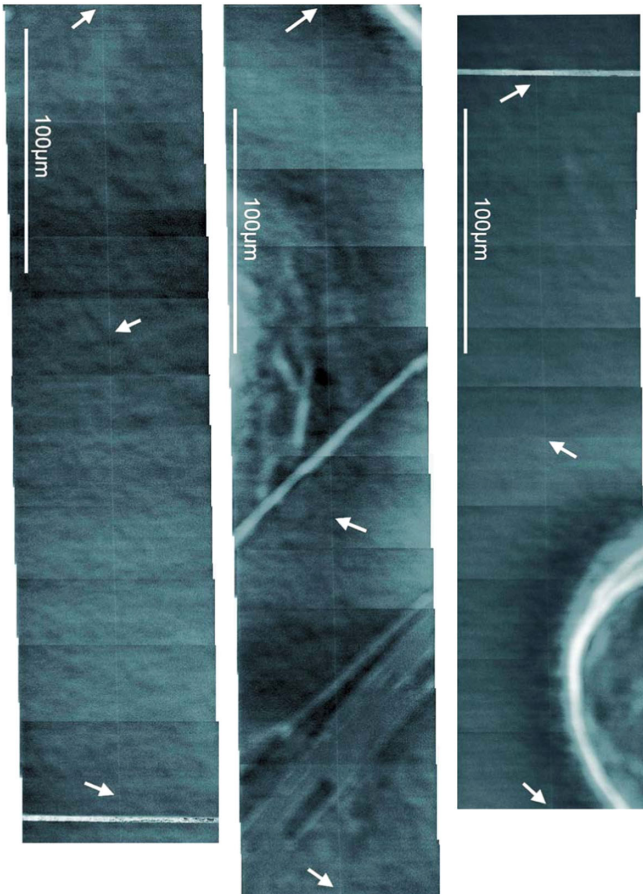


FIG. 2. SEM panorama of sample 9 (divided into three parts), where a CNT is suspended across a heater and a sensor (the horizontal beams in the top right and the bottom left images). The total suspended length of sample 9 is 1.039 mm. The arrows in the figures denote the CNT.

its relatively short L (< 30 μ m). For the longest CNT ($L = 1.039$ mm), $\kappa_m = 8638 \pm 734$ W/mK is measured (assuming $d = 2$ nm). Note that the effects of radiation heat loss from the CNT and contact thermal resistance have not been taken into account yet. Thus, $\kappa_m = 8638$ W/mK is a lower bound for the millimeter-long CNT.

Because of the radiation heat loss from the surface of the ultralong CNTs, the power received by the sensor is always smaller than that transmitted from the heater. Thus, the measured κ_m 's simply set the lower bound of the actual values. Moreover, because corrections from the radiation heat loss become more significant for longer L , they further enhance the divergent behavior of κ for ultralong CNTs [26]. We have analyzed the contribution of radiation heat loss and plotted the corrected values of κ 's. The divergent behavior is quantified using $\kappa \sim L^\alpha$. The α 's seem to vary from 0.1 to 0.5. However, for sample 6 ($L > 400$ μ m), sample 7 ($L > 400$ μ m), sample 8 ($L > 670$ μ m), and sample 9 ($L > 1$ mm) they are investigated over much larger length scales and may be closer to an ideal, disordered, quasi-1D system. Interestingly, their α 's are found to be 0.2–0.5, falling within theoretical predictions [9,13,14]. Notably, these α 's are smaller than previous results determined by micron-long, multiwall CNTs ($\alpha = 0.6$ –0.8) [23], indicating that the previous observation was mixed with conventional ballistic thermal conduction ($\alpha = 1$) of microscopic lengths. Note that after corrections from the radiation heat loss, the highest κ (assuming $d = 2$ nm) now respectively reaches 6900 W/mK for sample 5 ($L > 300$ μ m), 10 050 W/mK for sample 8 ($L > 670$ μ m), and 13 300 W/mK for sample 9 ($L > 1$ mm).

We now analyze the effect of contact thermal resistance. Because the contact areas ($\sim dw$, where d is the diameter of the CNT and $w = 2$ μ m is the width of a SiN $_x$ beam) between the CNT and each RT $_i$ are nearly identical for each sample, the contact thermal resistance ($1/K_c$) should be approximately a constant for individual CNTs and its effect can be analyzed in terms of a dimensionless quantity K_s/K_c , where K_s is the intrinsic thermal conductance of a 1 μ m-long CNT. So the measured thermal resistance ($1/K_m$) follows $1/K = (L/L_0)^{1-\alpha}/K_s + 1/K_c$, and the measured κ_m is expressed as

$$\kappa_m = \frac{K_s L}{\pi ds} \left(\frac{1}{(L/L_0)^{1-\alpha} + K_s/K_c} \right). \quad (4)$$

Here, $L_0 = 1$ μ m. To investigate the effect of the contact thermal resistance, we first assume that the CNT is an ordinary diffusive thermal conductor (i.e., $\alpha = 0$) and plot the result for different K_s/K_c 's in Fig. 4. From Fig. 4, it can be seen that although contact thermal resistance may yield spurious divergent behavior at short lengths, the curves always become flat for large L . Thus, the contact thermal resistance cannot explain the experimental data. Because the experimentally investigated L 's span 3 orders of magnitude yet the contact area remains the same, we

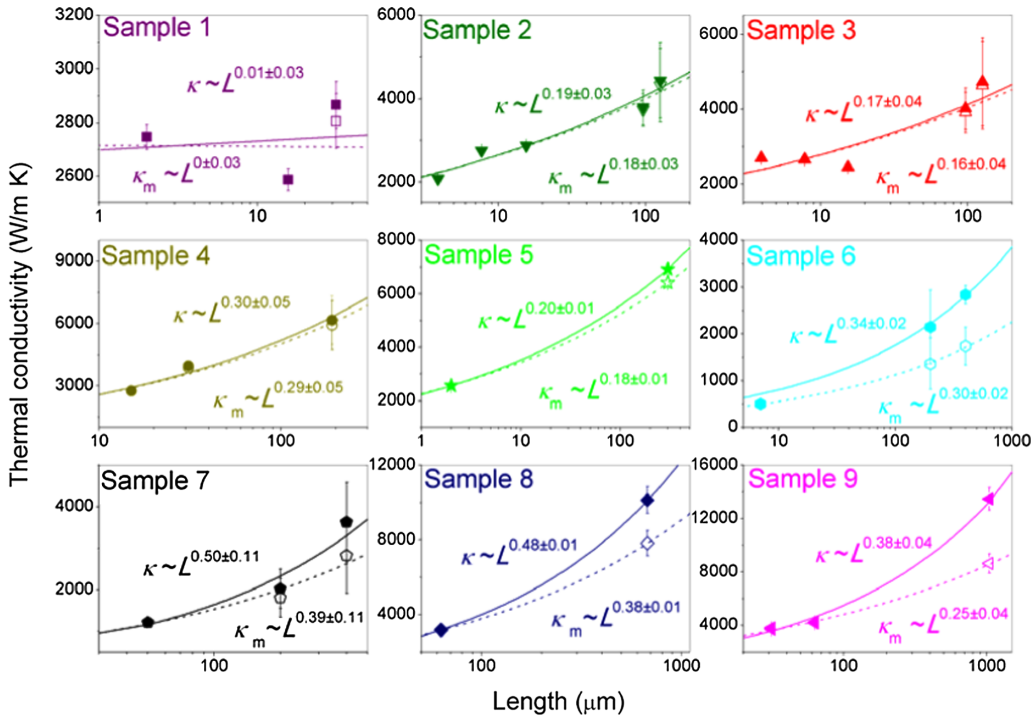


FIG. 3. κ vs L relations for nine different CNTs. Both measured κ_m 's (open symbols) and corrected κ 's (solid symbols, after incorporating radiation heat loss from the surface of CNTs) are shown for each sample. The measured κ_m 's and corrected κ 's are almost identical for $L < 100 \mu\text{m}$. For the longest CNT investigated ($L = 1.039 \text{ mm}$), the measured κ_m and the corrected κ reach 8640 and 13300 W/mK, respectively. The fits (by parametrizing $\kappa \sim L^\alpha$) to the corrected κ 's and measured κ_m 's are shown by solid curves and dashed curves, respectively.

have $L^{1-\alpha} \gg K_s/K_c$ in Eq. (4) and the effect of contact thermal resistance vanishes when $L \gg 1 \mu\text{m}$. Additionally, the effect of contact thermal resistance should be limited; for example, $K_s/K_c > 5$ would indicate that the intrinsic κ of a $1 \mu\text{m}$ -long CNT is larger than 18000 W/mK, violating quantum mechanical constraints for a CNT [28,29]. Further analyses using Eq. (4) suggest that $0.17 < \alpha < 0.43$ and $K_s/K_c < 0.3$ yield good fits to the experimental data [26]. Figure 4 also shows a controlled experiment on a SiN_x beam displaying the expected diffusive thermal conduction, demonstrating the validities of our measurements and analyses. Therefore, we conclude that the experimentally observed divergent behavior of κ originates from the intrinsic properties of the ultralong CNTs, but not from artifacts of contact thermal resistance.

Because naturally abundant ethanol vapor was used as the synthetic source, isotopic impurities (98.9% ^{12}C and 1.1% ^{13}C) are expected in the investigated CNTs. In addition, impurities and defects are unavoidable for the ultralong CNTs. Furthermore, TEM images reveal a thin layer ($\sim 2 \text{ nm}$) of amorphous carbon covering some parts of the CNTs [26]. Surprisingly, the pronounced power-law divergence of κ emerges regardless of these structural imperfections and external perturbations. The result is consistent with 1D disordered models that show robust anomalous thermal conduction phenomena against defects or disorders [5]. But it disagrees with the prediction that the divergent behavior of κ would disappear when defects are introduced in CNTs [9,16]. We thus demonstrate that the divergence of κ persists for much longer distances than theoretically anticipated [9,10,16]. Our results also resolve the decade-long debate of whether the κ of a CNT would

continue to diverge or saturate for $L > 1 \mu\text{m}$ [11–17]. The finding indicates that the wave properties of heat can be transmitted for much longer distances than previously thought, and it highlights the important contributions of long-wavelength phonons in low-dimensional systems.

Unlike electrical conductivity of materials that can vary by more than 27 orders of magnitude from insulators to metals,

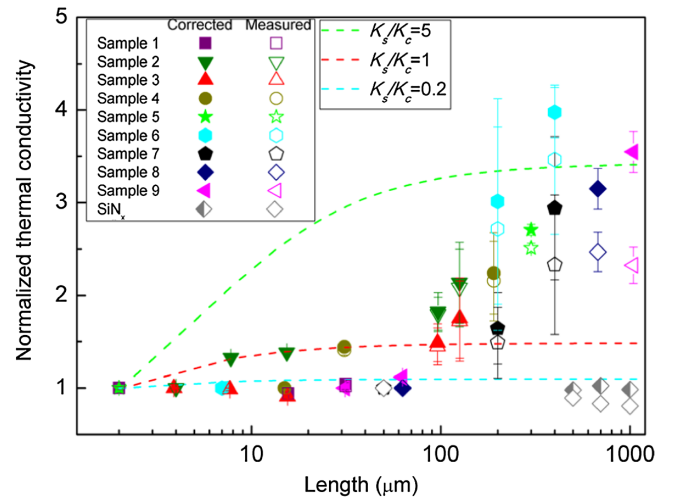


FIG. 4. Normalized κ vs L for the investigated samples. Here the corrected κ 's (solid symbols) and measured κ_m 's (open symbols) are normalized, respectively, by those of each sample's shortest L . The effects of contact thermal resistance from small ($K_s/K_c = 0.2$) to large ($K_s/K_c = 5$) are calculated using Eq. (4) (with $\alpha = 0$), demonstrating that the observed divergent of κ or κ_m cannot be attributed to contact thermal resistances adding to a diffusive thermal conductor. A controlled experiment on a SiN_x beam shows the expected normal thermal conduction.

κ 's were known to vary less than 10^5 from the best thermal conductors to the best thermal insulators in the past. The fundamental limitation has hampered most technological progress in directing heat or transmitting phonons. The divergent and ultrahigh κ observed in CNTs over 1-mm length scale could open a new domain for wave engineering of heat.

This work was supported by the Ministry of Science and Technology of Taiwan (MOST 104-2628-M-002-010-MY4).

V. L. and C.-H. W. contributed equally to this work.

*Corresponding author.

cwchang137@ntu.edu.tw

- [1] A. Dhar, *Adv. Phys.* **57**, 457 (2008).
- [2] K. Saito, S. Takesue, and S. Miyashita, *Phys. Rev. E* **54**, 2404 (1996).
- [3] S. Lepri, R. Livi, and A. Politi, *Phys. Rev. Lett.* **78**, 1896 (1997).
- [4] B. W. Li, H. Zhao, and B. B. Hu, *Phys. Rev. Lett.* **86**, 63 (2001).
- [5] A. Dhar and K. Saito, *Phys. Rev. E* **78**, 061136 (2008).
- [6] L. Yang, P. Grassberger, and B. Hu, *Phys. Rev. E* **74**, 062101 (2006).
- [7] K. Saito and A. Dhar, *Phys. Rev. Lett.* **104**, 040601 (2010).
- [8] L. Wang, D. He, and B. Hu, *Phys. Rev. Lett.* **105**, 160601 (2010).
- [9] N. Mingo and D. A. Broido, *Nano Lett.* **5**, 1221 (2005).
- [10] L. Lindsay, D. A. Broido, and N. Mingo, *Phys. Rev. B* **80**, 125407 (2009).
- [11] Z. H. Yao, J. S. Wang, B. W. Li, and G. R. Liu, *Phys. Rev. B* **71**, 085417 (2005).
- [12] D. Donadio and G. Galli, *Phys. Rev. Lett.* **99**, 255502 (2007).
- [13] G. Zhang and B. W. Li, *J. Chem. Phys.* **123**, 114714 (2005).
- [14] S. Maruyama, *Physica (Amsterdam)* **323B**, 193 (2002).
- [15] J. A. Thomas, R. M. Iutzi, and A. J. H. McGaughey, *Phys. Rev. B* **81**, 045413 (2010).
- [16] C. Sevik, H. Sevincli, G. Cuniberti, and T. Cagin, *Nano Lett.* **11**, 4971 (2011).
- [17] K. Saaskilanti, J. Oksanen, S. Volz, and J. Tulkki, *Phys. Rev. B* **91**, 115426 (2015).
- [18] D. L. Nika, A. S. Askerov, and A. A. Balandin, *Nano Lett.* **12**, 3238 (2012).
- [19] T. Prosen and D. K. Campbell, *Phys. Rev. Lett.* **84**, 2857 (2000).
- [20] T. Mai and O. Narayan, *Phys. Rev. E* **73**, 061202 (2006).
- [21] H. Hayashi, T. Ikuta, T. Nishiyama, and K. Takahashi, *J. Appl. Phys.* **113**, 014301 (2013).
- [22] H. Y. Chiu, V. V. Deshpande, H. W. C. Postma, C. N. Lau, C. Miko, L. Forro, and M. Bockrath, *Phys. Rev. Lett.* **95**, 226101 (2005).
- [23] C. W. Chang, D. Okawa, H. Garcia, A. Majumdar, and A. Zettl, *Phys. Rev. Lett.* **101**, 075903 (2008).
- [24] M. H. Bae, Z. Y. Li, Z. Aksamija, P. N. Martin, F. Xiong, Z. Y. Ong, I. Knezevic, and E. Pop, *Nat. Commun.* **4**, 1734 (2013).
- [25] X. F. Xu, L. F. C. Pereira, Y. Wang, J. Wu, K. W. Zhang, X. M. Zhao, S. Bae, C. T. Bui, R. G. Xie, J. T. L. Thong, B. H. Hong, K. P. Loh, D. Donadio, B. W. Li, and B. Ozyilmaz, *Nat. Commun.* **5**, 3689 (2014).
- [26] See Supplemental Material at <http://link.aps.org/supplemental/10.1103/PhysRevLett.118.135901>, which includes Refs. [27–35], for details of experimental methods and data analyses.
- [27] M. Hofmann, D. Nezich, A. Reina, and J. Kong, *Nano Lett.* **8**, 4122 (2008).
- [28] B. H. Hong, J. Y. Lee, T. Beetz, Y. M. Zhu, P. Kim, and K. S. Kim, *J. Am. Chem. Soc.* **127**, 15336 (2005).
- [29] S. M. Huang, X. Y. Cai, and J. Liu, *J. Am. Chem. Soc.* **125**, 5636 (2003).
- [30] L. X. Zheng, M. J. O'Connell, S. K. Doorn, X. Z. Liao, Y. H. Zhao, E. A. Akhadow, M. A. Hoffbauer, B. J. Roop, Q. X. Jia, R. C. Dye, D. E. Peterson, S. M. Huang, J. Liu, and Y. T. Zhu, *Nat. Mater.* **3**, 673 (2004).
- [31] T. L. Bergman, A. S. Lavine, and F. P. Incropera, *Fundamentals of Heat and Mass Transfer*, 7th ed. (Wiley, New York, 2011); M. Hofmann, D. Nezich, A. Reina, and J. Kong, *Nano Lett.* **8**, 4122 (2008).
- [32] T. K. Hsiao, H. K. Chang, S. C. Liou, M. W. Chu, S. C. Lee, and C. W. Chang, *Nat. Nanotechnol.* **8**, 534 (2013).
- [33] T. K. Hsiao, B. W. Huang, H. K. Chang, S. C. Liou, M. W. Chu, S. C. Lee, and C. W. Chang, *Phys. Rev. B* **91**, 035406 (2015).
- [34] R. Fainchtein, D. M. Brown, K. M. Siegrist, A. H. Monica, E. R. Hwang, S. D. Milner, and C. C. Davis, *Phys. Rev. B* **85**, 125432 (2012).
- [35] N. Mingo and D. A. Broido, *Phys. Rev. Lett.* **95**, 096105 (2005).